Refractive-Index Sensing With Inline Core-Cladding Intermodal Interferometer Based on Silicon Nitride Nano-Coated Photonic Crystal Fiber

Mateusz Smietana, Daniel Brabant, Wojtek J. Bock, *Fellow, IEEE*, Predrag Mikulic, and Tinko Eftimov

(Invited Paper)

***Abstract*—This paper presents a modification of the refractive-index (RI) response of an intermodal interferometer based on photonic crystal fiber (PCF) using a thin plasma-deposited silicon nitride (SiN_x) overlay with a high refractive index. We show that the film overlay can effectively change the distribution of the cladding modes and thus tune the RI sensitivity of the interferometer. Thanks to the nano-coating we were able to increase the RI sensitivity eightfold in the range required for biosensors ($n_D \sim 1.33$). Due to the extreme hardness of SiN_x films and their excellent adhesion to the fiber surface, we believe that after the film deposition the device will still maintain its advantages, i.e., lack of degradation over time or with temperature.**

***Index Terms*—Fiber-optic sensors, intermodal interference, optical fiber devices, photonic crystal fiber, refractive-index sensing, thin film.**

I. Introduction

A SIMPLE and cost-effective all-fiber structure based on intermodal interference between the core and cladding modes of a section of endlessly single-mode photonic crystal fiber (PCF) sandwiched between a lead-in and lead-out SMF-28 fiber has been intensively studied recently [1]–[6]. The interesting features of this structure are its compactness, the broad range of operation wavelengths, and its high stability over time. Its sensitivity to temperature, pressure, strain, bending and external refractive index (RI) has also been investigated. In such a structure, higher-order cladding modes of the PCF fiber are highly affected by the external medium, resulting in high RI sensitivity. Besides their RI sensitivity and simple fabrication, the structures offer low temperature-sensitivity (typically $\sim$5 pm/°C [2], [4]), and thus have two features that are highly desirable in the field of biosensing. Keeping in mind that the interferometers offer mainly relative measurements, the advantages of the PCF-based intermodal interferometers allow for treating them as more promising than Long-period Grating (LPG) or Fiber Bragg Grating (FBG) based devices, which show usually significant temperature cross-sensitivity or require complex fabrication procedures. However, the range of RI sensitivity does not appear to be suitable for biosensing applications, where sensitivity of around $n_D \sim 1.33$ is typically required [7]. Experimental results reported so far have shown that this type of interferometer offers high sensitivity in the RI range over $n_D \sim 1.4$ [2]–[4].

The deposition of high-refractive-index overlays of nanometric thickness has been shown to significantly modify the sensitivity of a number of optical fiber sensing structures to certain external influences [8], [9]. Various plasma-deposited films were applied in such structures for the first time by the authors of this paper [10]–[12]. In the present paper, we study the possibility of high-temperature radio-frequency (RF) plasma-deposition of silicon nitride (SiN_x) films on the SMF-PCF-SMF sensing structure. Due to their extreme hardness ($\sim$19 GPa) and excellent optical properties, SiN_x films typically find application as antireflective coatings for solar cells and as light-guiding layers in planar optical waveguide systems [13]. The films also exhibit a high refractive index (typically n from 2 to 3.5) and negligible absorption in the infrared spectral range, qualities which are required for optical sensors [14]. Due to their high n, even very thin SiN_x films are able to tune the RI sensitivity of the sensing structures [12].

II. Experimental Details

A 45-mm segment of endlessly single-mode fiber (Blaze Photonics ESM-12-01), with the polymer coating mechanically removed, was fusion-spliced (Ericsson FSU-975PM) between two lead-in and lead-out SMF28 fibers, following the procedure described in [2]. Deposition of the films was performed with the RF plasma-enhanced chemical-vapor-deposition (RF PECVD) Plasmalab 80+ system (Oxford Plasma Technology) working at a frequency of $f = 13.56$ MHz. The SiN_x films were deposited on samples suspended about 2.5 mm above the RF electrode and simultaneously on the wet oxidized silicon

Manuscript received July 26, 2011; revised October 14, 2011, October 28, 2011; accepted November 02, 2011. Date of publication November 08, 2011; date of current version March 16, 2012. This work was supported in part by the Natural Sciences and Engineering Research Council of Canada, in part by the Canada Research Chairs Program, NanoQuébec, and in part by the European Union in the framework of the European Social Fund through the Warsaw University of Technology Development Program.

M. Smietana is with the Institute of Microelectronics and Optoelectronics, Warsaw University of Technology, Warszawa 00-662, Poland (e-mail: M.Smietana@elka.pw.edu.pl).

D. Brabant, W. J. Bock, and P. Mikulic are with the Centre de recherche en photonique, Université du Québec en Outaouais, Gatineau, QC J8X 3X7, Canada (e-mail: brad06@uqo.ca; wojtek.bock@uqo.ca; predrag.mikulic@uqo.ca).

T. Eftimov is with the Faculty of Physics, Plovdiv University, Plovdiv 4000, Bulgaria (e-mail: teftimov@uni-plovdiv.bg).

Digital Object Identifier 10.1109/JLT.2011.2175201

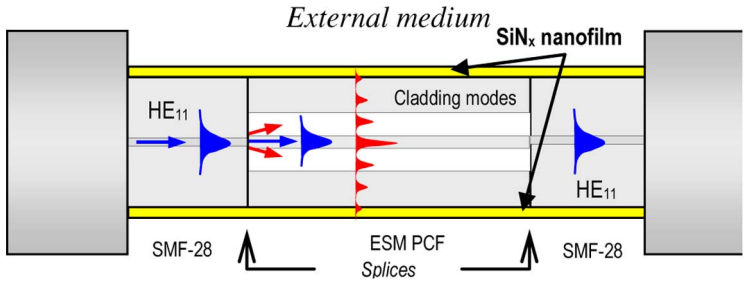

Fig. 1. Schematic representation of the PCF-based core-cladding intermodal interferometer nano-coated with a silicon nitride (SiN_x) overlay.

wafers used as reference samples, which in turn were placed directly on the electrode. The deposition procedure is similar to the one we previously reported [10]–[12]. We employed a high (SiH_4:N_2)/(NH_3) flow ratio (2% SiH_4 diluted in N_2) equal to 285/15 in order to obtain high-n SiN_x films. The other parameters for deposition were as follows: the RF power was 15 W, the pressure in the chamber was 0.53 mBar, the deposition time was from 5 to 9 minutes and the electrode temperature was from 300 to 325°C. The parameters of the films deposited on the reference samples, such as the refractive index (n), the extinction coefficient (k) and the thickness (t) were determined by a Horiba Jobin-Yvon UVISEL spectroscopic ellipsometer with a procedure described elsewhere [14].

For RI measurements, several mixtures of glycerin and water were prepared and their RIs (n_D) were determined using a VEE GEE PDX-95 refractometer working with an accuracy of $\pm 10^{-4}$ refractive index units (RIUs). The structures were kept under a constant tension and at a constant temperature during all the investigations. The response of the structure was monitored using an Agilent 86142B optical spectrum analyzer and an Agilent 83437A broadband light source. The schematic representation of the investigated structure is shown in Fig. 1.

Numerical simulations were performed using the FIMMWAVE software suites from Photon Design.

III. Results and Discussion

Thanks to the fusion splices between the SMF and PCF fibers and the collapsing holes in the short length of PCF, it is possible to independently excite the core and the higher-order modes in the PCF section (Fig. 1). Such modes propagate at different phase velocities, and at the second splice the modes interfere with an accumulated differential phase shift. Because of intermodal dispersion [2], the phase velocities and the phase difference are wavelength-dependent, the optical power transmitted in the device will show periodical changes versus wavelength as expressed in (1), where (I_{co}) and (I_{cl}) are the intensities of the core and cladding modes, (Δn_{eff}) is the difference between the effective refractive indexes of the core and cladding modes, and (L) is a length of the PCF segment. Since only the cladding modes are sensitive to the external environment, when the core mode propagates unperturbed, it is possible to detect variations in the external medium present on the surface of the PCF section.

$$T(\lambda) = I_{co}(\lambda) + I_{cl}(\lambda) + 2\sqrt{I_{co}(\lambda)\cdot I_{cl}(\lambda)}\cdot\cos\frac{2\Pi\cdot\Delta n_{eff}\cdot L}{\lambda} \quad (1)$$

A. Experimental Results

The t of the films deposited (at $\lambda = 1560$ nm) on the reference samples was determined to be from 50 to 85 nm and the n, from 2.27 to 2.44. The increase in the films' n with their t has been discussed elsewhere [13]. Measurements in the present work established that films show a negligible k in the infrared spectral range. The effect of the variations in external RI within a narrow range (n_D from 1.332 to 1.342) for a sample without nano-coating and selected samples with coating is compared in Fig. 2. The spectral range has been selected arbitrarily in order to clearly show the variations in the interference pattern.

When there is no coating on the fiber, the shift of the interference is higher when the external index gets closer to that of the fiber (Fig. 3). Above that value, the cladding mode becomes a radiation mode and the interference pattern disappears. At a certain t and n of the nano-coating, as the external RI increases, an increase can be seen in the visibility of the fringes (Fig. 2(c)). We believe that the interference pattern experiences a shift of over one period, due to the presence of the nano-coating. The relation between the sensitivity and the film properties is not straightforward. For films that are 53 nm thick and have an n of 2.31, we were able to increase the device sensitivity 8 times over that of the sample with no coating in the external RI range around $n_D \sim 1.33$. It can be seen that both the t and the n of the coating must be precisely adjusted in order to optimize the RI sensitivity of the device (Fig. 3).

B. Simulation Results

As show above, when the film is deposited, the interference patterns experience a higher wavelength shift than does the sample with no coating. The effect is observed due to the fact that when the nano-coating is deposited on the PCF segment, the effective indexes of the cladding modes increase, simultaneously increasing the Δn_{eff}. The increased sensitivity due to the presence of the overlay can also be explained by the corresponding shift in the energy of the cladding modes toward the radial edge of the device. The resulting interference distribution of the modes inside the PCF structure presents more light energy toward the radial edge, thus increasing its susceptibility to the sensed media. Fig. 4 displays the simulated radial interference pattern at the end of the PCF fiber without the overlay (Fig. 4(a)) and with an overlay having a t of 65 nm (Fig. 4(b)). The inference pattern at the end-face of a 45-mm length of ESM PCF fiber was obtained from the propagation of the first 50 modes (core mode +49 cladding/overlay modes)

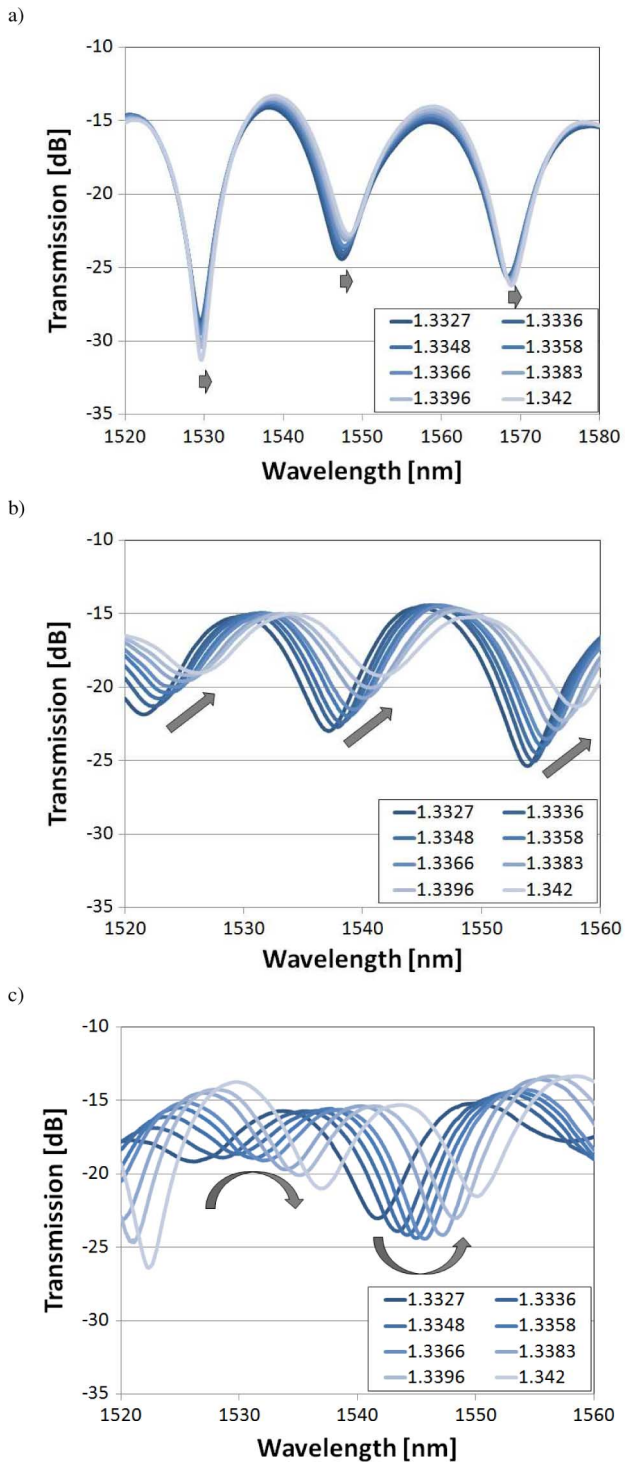

Fig. 2. Spectrum evolution induced by changes of external RI in the range from 1.332 to 1.342 in three samples: (a) bare sample, (b) S5 ($t = 58$ nm; $n = 2.31$) and (c) S7 ($t = 53$ nm; $n = 2.31$).

along the fiber. A higher density of energy toward the radial edge of the fiber is clearly visible for the nano-coated fiber.

In order to further correlate the experimental results with computer simulations, we modeled the PCF component using the improved effective-index method (IEIM) described in detail in [15]. With the IEIM, a PCF is accurately modeled as a simple standard step-index fiber (SIF), where the core radius (ρ_{core})

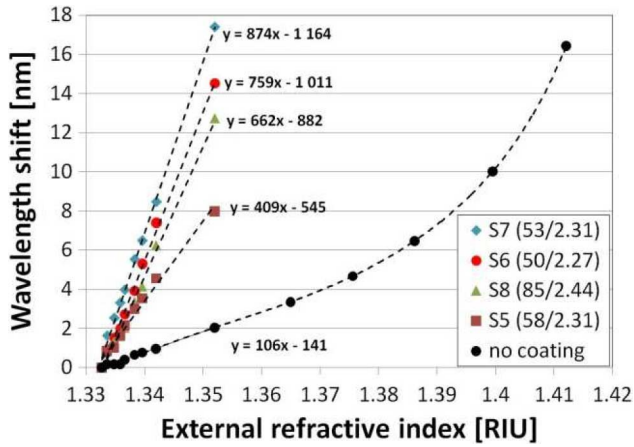

Fig. 3. Sensitivity to changes in external RI for samples coated with SiN_x film of different t and n. The t is given in nm and the n is determined at $\lambda = 1560$ nm.

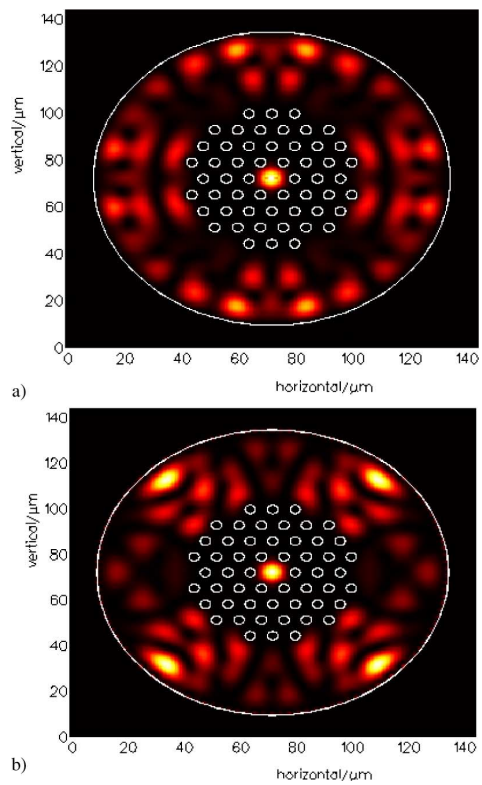

Fig. 4. Simulated interference distribution at the end-face of the PCF fiber ($L = 45$ mm, external RI of 1.332, and $\lambda = 1550$ nm): (a) with no overlay and (b) with an overlay of predetermined $t = 65$ nm ($n = 2.31$).

is calculated as in (2), where $c_1 = 0.68064$, $c_2 = 0.265366$, $c_3 = 1.291080$, d is the diameter of the PCF holes, and Λ is the PCF pitch. Using the information found in the ESM-12-01 PCF datasheet, we have computed an effective core radius value of $\rho_{\text{core}} = 5.259019$ μm

$$\rho_{\text{core}} = \frac{c_1 \Lambda}{1 + \exp\left[\frac{\left(\frac{d}{\Lambda} - c_3\right)}{c_2}\right]}. \tag{2}$$

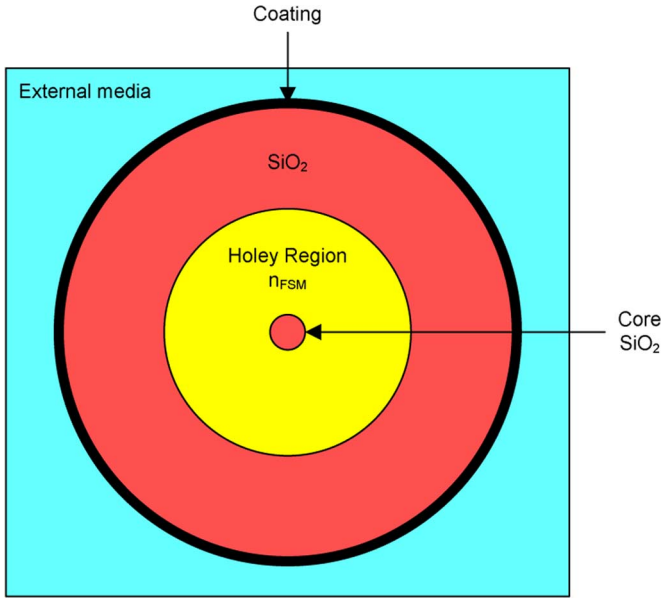

Fig. 5. Five-layer structure of the SIF used to model a coated ESM-12-01 PCF.

The index of pure silica and the index of the fundamental space-filling mode (FSM) of the corresponding PCF fiber are used as the respective indexes of the core and cladding SIF model. The index of the FSM for the ESM-12-01 PCF was calculated in the wavelength range of interest (λ from 1500 to 1600 nm) using the finite-element based mode solver of FIMMWAVE. The dispersion of the FSM was then modeled using the fitting curve expressed in (3), where $a_0 = 1.464732$, $a_1 = -0.0149$, and the λ is given in μm

$$n_{\mathrm{FSM}}(\lambda) = a_0 + a_1\lambda. \tag{3}$$

The coated ESM-12-01 PCF in an external medium was modeled as the SIF five-layer structure illustrated in Fig. 5. The core, cladding, and coating modes of that structure were then computed using the finite-difference based mode solver available in FIMMWAVE. Finally, the propagation simulation along the SMF-PCF-SMF device was performed using the FIMMPROP modeling tool available in the FIMMWAVE software suite. The propagation algorithm of the FIMMPROP tool is the Eigenmode Expansion Method [16].

It should be noted that the splice regions between the SMF-28 fiber and the PCF were not modeled per se. Instead, the input to the PCF was taken as a broad Gaussian beam (15 μm FWHM) in order to model the collapsing of the PCF holes due to splicing. The interface between the PCF and the output SMF-28 fiber in our propagation model did not consider the effects resulting from the splicing process. The output of the system was simply taken as the total power coupled to the fundamental mode of the SMF-28 fiber.

The model approximation at the first interface is the cause of the shallower interference pattern in the simulated transmission spectrums. The input Gaussian beam is believed to generate more energy in the core mode of the modeled PCF than the actual splicing does and thus to reduce the interference pattern contrast as can be assessed from (1). The approximation

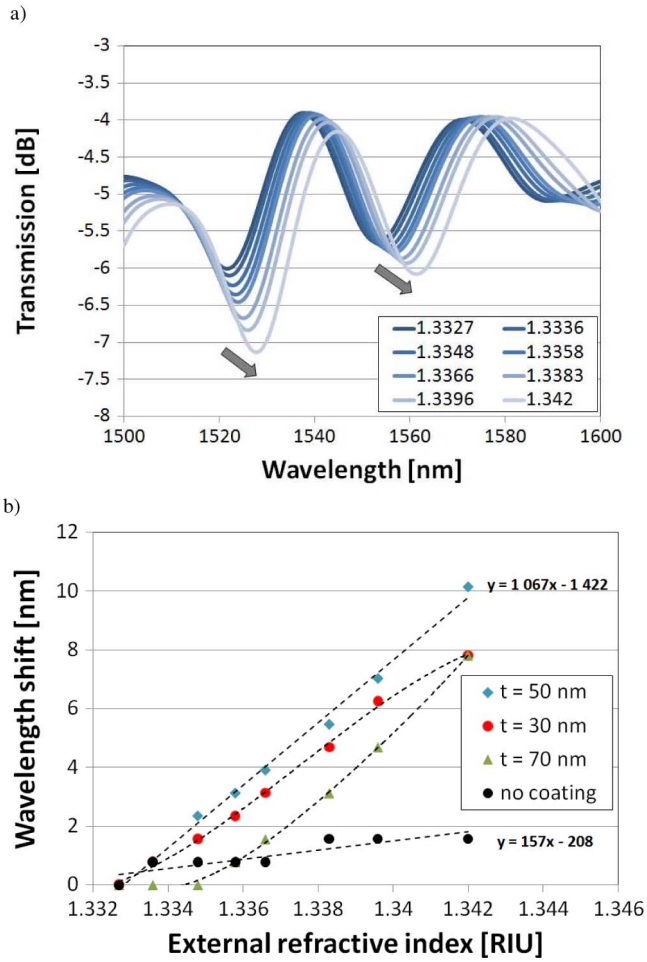

Fig. 6. Results of the simulations showing influence of changes of external RI in the range from 1.332 to 1.342, where (a) is an interference pattern when $t = 50$ nm and (b) is sensitivity-dependent on t. Simulations were performed for $n = 2.31$.

made at the second interface of the device results in simulated transmission spectrums with larger values than those found experimentally. This is due to the collapse of the PCF holes caused by the splicing which results in the excitation of leaky modes in the output SMF-28 fiber which will leak out. This effect is not taken into account in our model. However, it is the authors' belief that those limitations do not affect the modeling of the observed effects and improved sensitivity due to the coating layer on the device.

For simulation purposes we assumed the n of the nano-coating to be 2.31, and the t to be 30, 50 and 70 nm. The obtained interference pattern is illustrated in Fig. 6(a). The significant influence of the external RI on the interference pattern is evident. The wavelength shift is strongly dependent on the coating properties, and has its highest values when the thickness is around 50 nm for $n = 2.31$. The obtained simulation results are in good agreement with the measurements.

IV. Conclusion

A plasma-deposited thin SiN_x overlay can effectively modify the RI sensitivity of a PCF-based intermodal interferometer. Thanks to this nano-coating we were able to increase the RI

sensitivity eightfold in the range typically required for biosensors. We found that both the thickness and the refractive index of the coating must be precisely adjusted in order to optimize the RI sensitivity of the device. We believe that due to its extreme hardness and excellent adhesion to the fiber surface, the SiN_x overlay will enable the device to maintain its robustness, i.e., there will be no degradation of its properties over time or with temperature.

REFERENCES

[1] H. Y. Choi, M. J. Kim, and B. H. Lee, "All-fiber Mach–Zehnder type interferometers formed in photonic crystal fiber," *Opt. Exp.*, vol. 15, pp. 5711–5720, Apr. 2007.

[2] W. J. Bock, T. A. Eftimov, P. Mikulic, and J. Chen, "An inline core-cladding intermodal interferometer using a photonic crystal fiber," *J. Lightw. Technol.*, vol. 27, no. 9, pp. 3933–3939, Sep. 2009.

[3] R. Jha, J. Villatoro, G. Badenes, and V. Pruneri, "Refractometry based on a photonic crystal fiber interferometer," *Opt. Lett.*, vol. 34, pp. 617–619, Mar. 2009.

[4] J. Villatoro, V. Finazzi, G. Badenes, and V. Pruneri, "Highly sensitive sensors based on photonic crystal fiber modal interferometers," *J. Sens.*, vol. 2009, p. 747803, May 2009.

[5] Y. Geng, X. Li, X. Tan, Y. Deng, and Y. Yu, "A cascaded photonic crystal fiber Mach Zehnder interferometer formed by extra electric arc discharges," *Appl. Phys. B*, vol. 102, pp. 595–599, Sep. 2010.

[6] J. Villatoro, V. P. Minkovich, V. Pruneri, and G. Badenes, "Simple all-microstructured-optical-fiber interferometer built via fusion splicing," *Opt. Exp.*, vol. 15, pp. 1491–1496, Feb. 2007.

[7] M. E. Bosch, A. J. R. Sanchez, F. S. Rojas, and C. B. Ojeda, "Recent development in optical fiber biosensors," *Sensors*, vol. 7, pp. 797–859, Jun. 2007.

[8] F. J. Arregui, I. R. Matias, J. M. Corres, I. Del Villar, J. Goicoechea, C. R. Zamarreno, M. Hernaez, and R. O. Claus, "Optical fiber sensors based on layer-by-layer nanostructured films," *Procedia Eng.*, vol. 5, pp. 1087–1090, Sep. 2010.

[9] M. Smietana, W. J. Bock, J. Szmidt, and G. R. Pickrell, "Nanocoating enhanced optical fiber sensors," *Ceramic Trans.*, vol. 222, pp. 275–286, Dec. 2010.

[10] M. Smietana, J. Szmidt, M. Dudek, and P. Niedzielski, "Optical properties of diamond-like cladding for optical fibres," *Diamond Related Mater.*, vol. 13, pp. 954–957, Apr./Aug. 2004.

[11] M. Smietana, M. L. Korwin-Pawlowski, W. J. Bock, G. R. Pickrell, and J. Szmidt, "Refractive index sensing of fiber optic long-period grating structures coated with a plasma deposited diamond-like carbon thin film," *Meas. Sci. Technol.*, vol. 19, p. 085301, Jun. 2008.

[12] M. Smietana, W. J. Bock, P. Mikulic, and J. Chen, "Pressure sensing in high-refractive-index liquids using long-period gratings nanocoated with silicon nitride," *Sensors*, vol. 10, pp. 11301–11310, Dec. 2010.

[13] L. Martinu and D. Poitras, "Plasma deposition of optical films and coatings: A review," *J. Vac. Sci. Technol. A*, vol. 18, pp. 2619–2645, Nov./Dec. 2000.

[14] M. Smietana, W. J. Bock, and J. Szmidt, "Evolution of optical properties with deposition time of silicon nitride and diamond-like carbon films deposited by radio-frequency plasma-enhanced chemical vapor deposition method," *Thin Solid Films*, vol. 519, pp. 6339–6343, Apr. 2011.

[15] K. N. Park and K. S. Lee, "Improved effective-index method for analysis of photonic crystal fibers," *Opt. Lett.*, vol. 30, no. 9, pp. 958–960, May 2005.

[16] D. F. G. Gallagher and T. P. Felici, "Eigenmode expansion methods for simulation of optical propagation in photonics—Pros and cons," in *Proc. SPIE*, Jan. 2003, vol. 4987, p. 69.

M. Smietana received the B.Sc., M.Sc., and Ph.D. degrees (with distinction) in electronics from the Warsaw University of Technology (WUT), Poland, in 2000, 2002, and 2007, respectively.

Since March 2007, he has been an Assistant Professor in the Institute of Microelectronics and Optoelectronics, WUT. He was a postdoctoral fellow at Virginia Tech and Université du Québec en Outaouais (UQO), Canada. He received scholarships from the European Social Fund through the WUT Development Programme (Poland) and from the FQRNT by the Ministère de l'Éducation, du Loisir et du Sports du Québec (Canada). His fields of interest are fiber-optic sensors and thin films.

D. Brabant received the B.Sc. degree in physics in 1990 and the M.Sc. degree in computational physics in 1992 from Université de Montréal, QC, Canada.

From 1993 to 2008, he worked in the private industry and in the public sector where he specialized in the development of simulation software for all-fiber and electro-optic components. In 2007, he was awarded a High Performance Computing Virtual Laboratory scholarship from Sun Microsystems of Canada.

Wojtek J. Bock (M'85–SM'90–F'03) received the M.Sc. degree in electrical engineering and the Ph.D. degree in solid state physics from Warsaw University of Technology, Poland, in 1971 and 1980, respectively.

Since 1989, he has been a Full Professor of Electrical Engineering at the Université du Québec en Outaouais (UQO), Canada. Since 2003, he has held a Canada Research Chair Tier-I in Photonics and has been Director of the Photonics Research Center at UQO. His research interests include fiber-optic sensors and devices, multisensor systems, and systems for precise measurement of non-electric quantities. He has authored and co-authored more than 270 scientific papers, patents and conference papers in the fields of fiber optics and metrology which have been cited about 300 times.

He is an Associate Editor of the IEEE/OSA JOURNAL OF LIGHTWAVE TECHNOLOGY and the *International Journal of Optics*.

P. Mikulic received an Associate of Science Degree as a Telecommunication Engineering Technologist from the University of Sarajevo, Yugoslavia in 1989.

He has more than 20 years of professional high-tech experience in the industry. His major interests are thin-film deposition, excimer lasers, photonic devices, fiber sensors, and procedures for splicing dissimilar fibers including photonic crystal fibers.

T. Eftimov received the M.Sc. degree in quantum electronics from Sofia University, Sofia, Bulgaria, in 1982 and the Ph.D. degree in applied physics from the Technical University of Sofia, in 1989.

He is currently with the Department of Experimental Physics, Plovdiv University, Plovdiv, Bulgaria. His interests include optical fibers, polarization phenomena, intermodal interference, fiber gratings, and fiber-optic sensors. In these fields he has authored and co-authored more than 80 journal and conference papers.